THE UNIVERSITY OF NEW MEXICO

DEPARTMENT OF PHYSICS AND ASTRONOMY

FINAL REPORT

for

NASA Research Grant NGR 32-004-036

and

Supplement No. 1 NGL 32-004-036

April 1, 1968 to November 30, 1971

ALBUQUERQUE, N. M.

THE UNIVERSITY OF NEW MEXICO
Department of Physics and Astronomy

FINAL REPORT

for

NASA Research Grant NGR 32-004-036
and
Supplement No. 1 NGL 32-004-036

April 1, 1968 to November 30, 1971

by

Alan W. Peterson

Principal Investigator

February 1972

CONTENTS

Figures

Appendices

Recent Papers

Summary

This report summarizes a program of infrared studies of the circumsolar and night sky conducted between April, 1968, and November 30, 1971, at the University of New Mexico. In addition to observations performed at Capillo Peak Observatory in New Mexico, airborne observations from the Ames Research Center's CV990 were performed in 1968, and eclipses in Siberia (1968) and southern Mexico (1970) were observed with NSF support.

Two dual-channel filter photometers covering wavelengths in the 0.8 to 4.8 μ range were constructed for the aircraft and eclipse observations. A single channel differential photometer was constructed for daytime circumsolar observations. Two large-aperture (12 inch and 24 inch) photometers have been constructed for twilight and night sky photometry. Finally, a small spectrograph for eclipse work has been constructed. It has been used for airglow observations also.

Other specialized instrumentation include a four-axis mounting for radial scanning with the eclipse photometers and a 14-inch diameter collimator for use with a black body in calibration of the photometers.

Observations performed include:

a. Ten solar flights on the CV990 in the summer of 1968

b. Two solar eclipse expeditions

c. Two observing trips to Haleakala, Hawaii, for day, twilight, and nighttime work.

d. Over 100 trips to Capillo Peak Observatory for day, twilight, and nighttime work.

Significant observations and results include:

a. Verification of the impossibility of making coronagraphic observations from inside an aircraft which are less contaminated with scattered light than ground based measurements.

b. Analysis of New Mexico infrared aureole data which requires inclusion of particles as large as 70 μ for proper theoretical fitting of the data.

c. Detection of fluctuations in the OH airglow at 2.2 μ of amplitude up to 5%. These correspond to "cells" of linear size ~100 km and with lifetimes ~½ hour.

d. Finding rather reproducible, but not accurately measureable peaks at 4 R_{o} in daytime measurements at Haleakala; presumably these are due to dust emission near the sun.

e. Obtaining a submicron measurement (0.84 and 0.96 μ) of the 4 R_{o} dust emission peak at the 1970 eclipse.

f. Making a first vaporization temperature measurement of the 4 R_{o} dust using data at three wavelengths from the 1970 eclipse. This value is 2160±200°K.

g. Devising a means to retrieve data which was recorded "oversmoothed."

h. Using a Hewlett-Packard PIN photodiode for eclipse measurements in the near infrared.

i. Using scans of red twilight rays to deduce and verify the height of the sulphate aerosol layer as 19.5±0.5 km and to verify that infrared twilight ceases at a solar depression angle of 11° instead of 18° as in the visible.

I. Introduction

The concept of thermal emission was advocated around the turn of the century to explain the solar corona's continuous spectrum as due to incandescent meteoric material. Such theories never went beyond calculating a black-body temperature for a specified distance from the sun. These models were superceded by the electron gas model (the K-corona) which, in turn, was modified by addition of a dust-scattered component (the F-corona). Even though numerous observations indicated an excess of red light in the outer corona the possible role of thermal emission by circumsolar dust was never considered as a source of coronal reddening. The latter was presumably adequately explained by diffraction.

In 1961 the writer made the first explicit calculations of the expected magnitude of a thermal emission component from the zodiacal dust cloud. Later in 1963 these calculations had been extended into the corona and specifically applied to the region where the dust approaching the sun is vaporized. A definite signature of the dust emission would be an infrared spike, sharp on the inner edge, at some distance from the sun which would be set by the dust vaporization temperature. In addition, it appeared that this emission might be detected in broad daylight with near-sun infrared observations.

On September 3, 1966, a peak at 4 R_o was observed for the first time in a series of daylight infrared measurements near the sun. Later at the November 12, 1966 eclipse in Bolivia, symmetrically placed peaks were observed at 4 R_o in the outer corona. Since these first positive results the emphasis has been to extend the observations to a large wavelength range, to determine the dust vaporization temperature, and to study the role of dust emission in any possible coronal reddening. In addition, if thermal emission could be observed at large distances from the sun, the space density of the zodiacal dust would be directly obtainable. We now discuss the various observations which have been attempted in support of these ideas.

II. Observational Programs

A. Multiwavelength Infrared Scans of the Circumsolar Sky from the Ames CV990 Flying Laboratory.

When support was made available in April, 1968, it was with the stipulation that the first observations were to be made during the summer series of flights of the Ames CV990. In addition, we were informed that open port observations were impossible from this aircraft. Thus with the strong suspicion that nothing of value would come from the observations because of the scattering from the entrance window, we went ahead and designed and constructed a dual-channel infrared coronagraph for use onboard the CV990.

The photometer consisted of PbS and InSb detectors cooled by cryostat-generated liquid nitrogen. A single chopper interrupted both incoming beams which were separated by 1.375 inches. The optical systems were 0.6 inch diameter 1.5 inch focal length quartz or sapphire lenses looking through 1-inch diameter interference filters. The chopper was contained in a dry-ice cooled chamber.

A four knife edge occulting system was calculated to scatter less than 10^{-7} B_o over the entrance window at an elongation angle of 3.0 R_o. The occulting system was carried on a channel-iron spar five feet long. A mounting permitted rotation of the photometer and spar about the aircraft axis.

Motor driven scanning motion was perpendicular to the aircraft axis. A stabilized mirror provided a beam of sunlight accurately parallel to the aircraft axis.

In order to make observations at the 5.3 μ limit of the InSb detector a sapphire entrance window 4.5-inches in diameter was first used. This proved to be unsatisfactory because of the large scatter from the internal striations in the sapphire. The latter was flame grown and exhibited much radial structure due to the stream line flow of the gases around the front of the growing crystal. In addition the 1-inch diameter central seed crystal was clearly visible in direct sunlight.

For the second series of flights the instrument was moved amidships to lessen vibration, which was a problem in our first tail location. In addition, a 12x14 inch quartz window was provided by Ames. With a quartz window observations at wavelengths greater than 3.5 μ were precluded. While the observations now appeared promising we still did not know what the absolute brightnesses were which we were measuring since we had had no time to calibrate the instrument before the flights. Only later did the large brightness values become apparent after the photometer was calibrated and corrections were made for the absorption in the thick quartz window.

Results and Conclusions

In Figure 1 we present the brightness of the circumsolar sky as observed from the ground in New Mexico and in Hawaii and from the CV990. The wavelength was 2.23 μ. The data are corrected to the zenith although this is not a meaningful correction for the aircraft data since these are mainly window scatter. In New Mexico the aureole is generally bright and easily detectable in the visible. In Hawaii the aureole is normally very faint and frequently not detectable at all in the visible. It is noteworthy that the Hawaii data are a factor of four fainter than the CV990 data at $E = 1^{o}$ and a full order of magnitude fainter at $E = 2^{o}$.

The small bump in the Haleakala data between 1.1 and 1.25^{o} is presumably dust emission. Its magnitude $\sim 5 \times 10^{-9}$ B_o is higher than that measured in eclipses where values of 1 to 2×10^{-9} B_o are obtained.

The New Mexico data correspond to an average day when the sky is bright and the aureole readily visible and white in color.

We conclude that the aircraft data give smaller sky brightnesses than average conditions in New Mexico but they are very inferior to the measurements easily obtainable in Hawaii. Indeed the shape of the Hawaii aureole suggests strongly that the major contribution is from diffraction by the occultings system and not from the solar aureole.

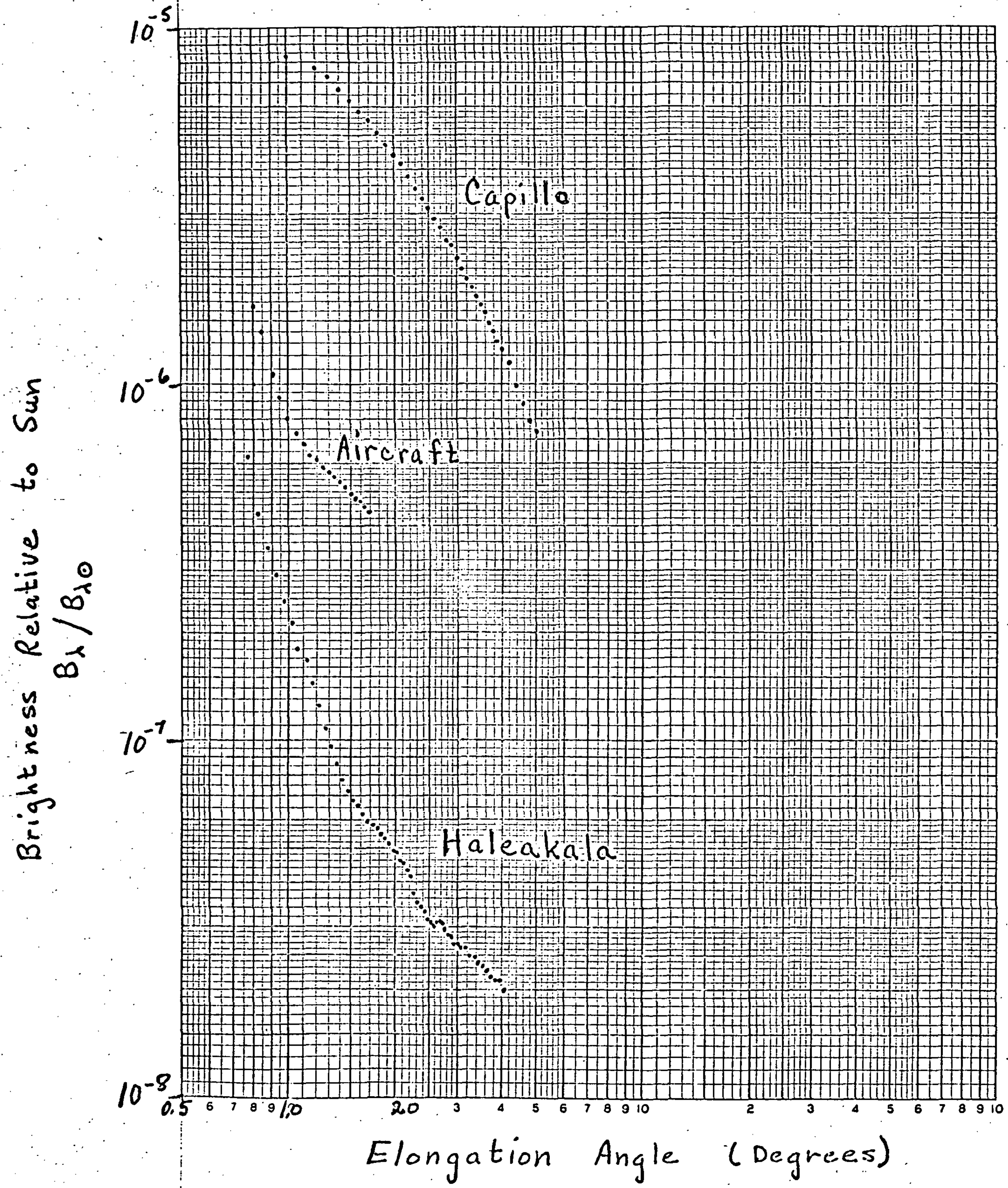

Fig. 1 Comparison of aureole measurements.

B. Ground Based Observations

Initial attempts to detect circumsolar dust emission were made in New Mexico in 1965 under General Dynamics/Fort Worth sponsorship. The instrument was a 12-inch telescope directed at the meridian and shaded by a 5x10 foot sheet of plywood supported horizontally at the top of a 60 foot tower. These measurements were continued the next summer using a 6-inch telescope when the writer was at the University of Missouri. It was with the externally occulted 6-inch telescope that the first definite evidence of an infrared spike at 4 R_o was obtained on September 3, 1966. This faint and peculiar aureole occurred after a rainy spell of four days. It is shown in Figure 2 as observed at $\lambda = 3.61\ \mu$ and we consider the small bump at 1.1^o elongation to represent the first observation of circumsolar dust emission. The aureole between 1 and 2^o elongation was only faintly visible at this time. The atmosphere presumably contributes $\sim 10^{-7}$ B_o of thermal emission at this wavelength. In the summer of 1967 by far the most aureole data were collected with an externally diaphramed heliostat 70 feet from the 6-inch telescope. With this set up continuous aureole recordings could be made during the entire day. A set of such observations for September 3, 1967 is given in Figure 3. It is apparent that during average summer weather when bright aureoles predominate, the search

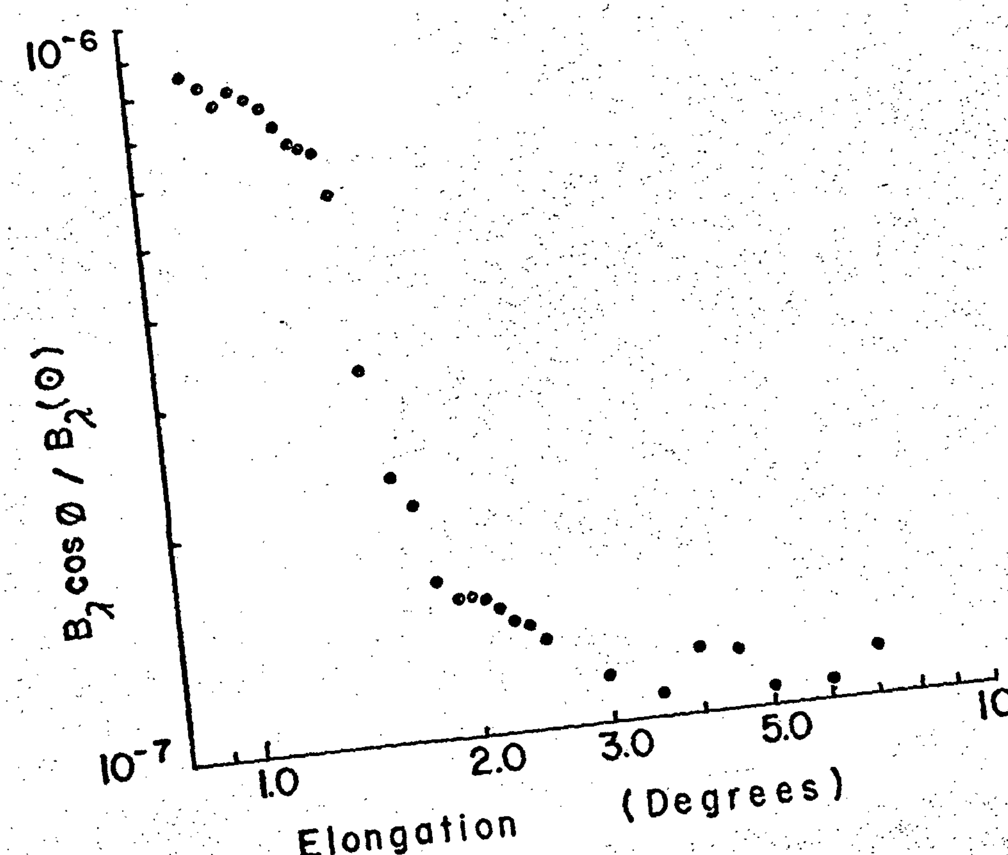

Fig. 2 The very faint aureole of 9/3/66 showing a small bump at E = 1.1°, which is presumably dust emission near the sun.

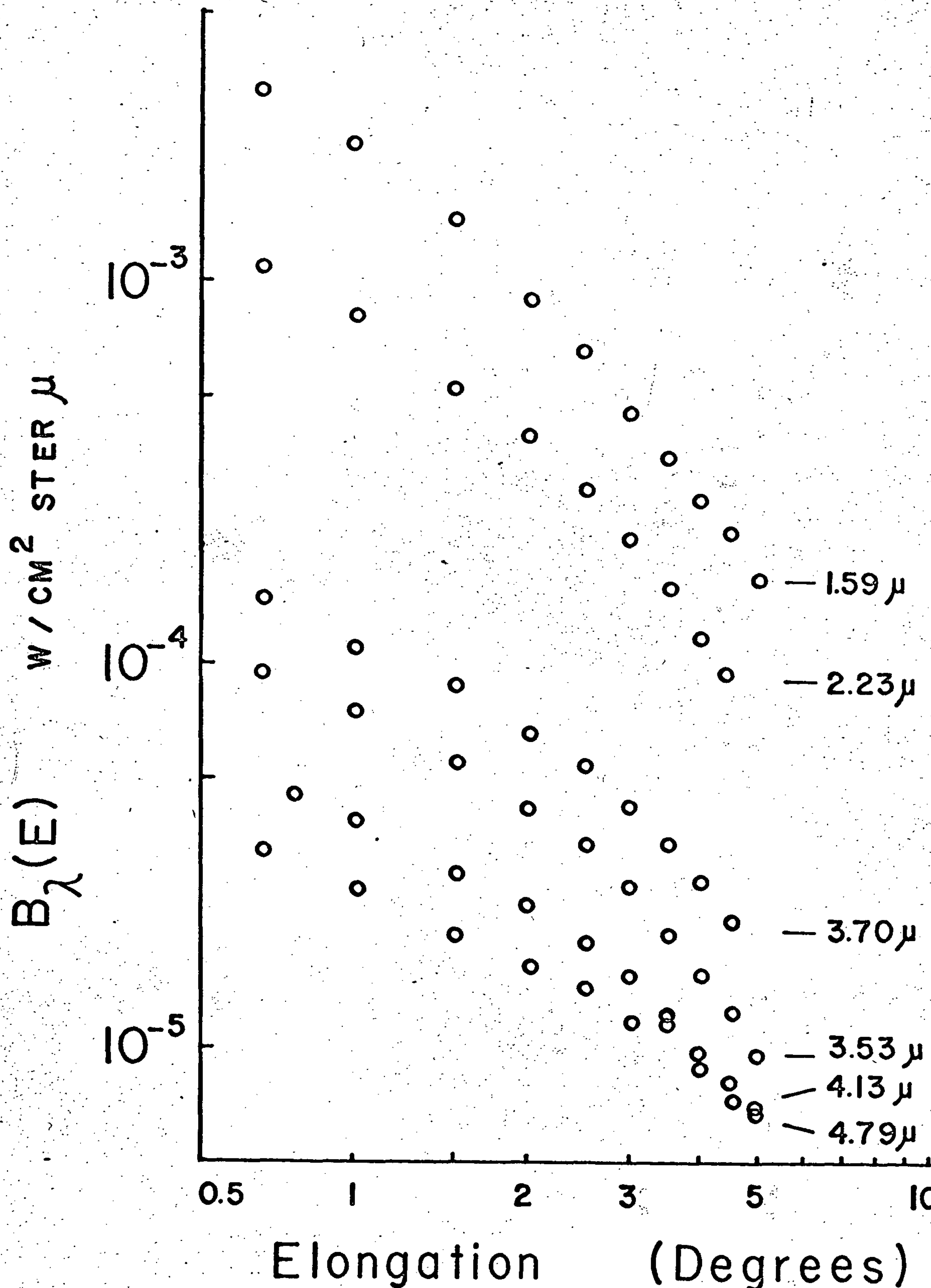

Fig 3 A set of multiwavelength aureole measurements in the infrared. The sky was somewhat brighter than average when this data was taken.

for thermal emission peaks is pointless. However the aureole data provide significant information on atmospheric dust. In particular one obtains information on the large particles in the aerosol population. The usual discussions of atmospheric aerosols terminate at a maximum particle size ~2 μ. This is due, primarily, to the fact that such particles are strongly forward scattering and do not contribute significantly to the aureole at readily measurable distances from the sun. With infrared measurements a 2 μ particle has its forward scattering lobe extending to 37°.5 from the sun at λ = 2 μ whereas at λ = 0.5 μ the lobe extends out to only 8°.6. For a 20 μ particle its forward scattering is confined to a cone only 0.4° at λ = 0.5 μ and is thus unobservable with usual aureole techniques whereas at λ = 2 μ the scattering lobe extends to 1°.6 from the sun and is thus observable.

Two papers were written on the analysis of infrared aureole observations but have not yet been published. Our average aureole in New Mexico requires particles as large as 70 μ in radius to reproduce the observations. A good fit is obtained only for an exponential radius distribution with the exponent equal to 3.56. The infrared observations specify this parameter quite precisely. Our integrated number of particles in a 1 cm^2 column agrees quite well with other published values. The number of particles with radius ~70 μ is only ~10^{-2} cm^{-2} column.

The source of such large particles seems to be somewhat of a mystery. However the most likely source is coal burning power plants in northwest New Mexico which are known to inject from 300 to 400 tons of fly ash per day into the atmosphere. These dust plumes have been photographed from space. They have also been visually detected from aircraft and traced back to the source from Los Alamos.

An uncompleted experiment on the aureole was to attempt nighttime stellar aureole measurements to determine the diurnal variation of atmospheric dust.

The Heleakala data on the aureole seem to be contaminated with too much diffracted light from the knife edge occulter to yield meaningful aureole models. When an improved occulter is put into operation we hope to specify the large particle segment of the aureole distribution over Hawaii.

C. Eclipse Observations of 1968 and 1970

The total solar eclipse of September 22, 1968 was observed from Yurgamysh, Kurgan, USSR in western Siberia. The dual channel aircraft photometer and a single channel unit were used.

Pre-eclipse weather was very depressing with the sun not visible for the entire week. Thus no realistic practice runs or calibrations were possible. During the late evening before the eclipse the sky cleared. Scattered fair weather cumulus developed on eclipse day. Hurried collimations were made and a few aperture stop calibrations run. At eclipse time the sky was essentially cloud free.

We recorded the sky brightness decline near totality at ~10 R_o south of the sun on the solar almucantar. Some 35 seconds before totality a large increase in sky brightness was recorded (~x5). Then at 10 seconds before totality another large increase was recorded which lasted almost 20 seconds. Thus at the start of totality the sky was actually brighter at 10 R_o than it had been 20 seconds earlier. Another anomaly was a large and persistent Bailey Bead on the sun's eastern limb which endured some 10 seconds after totality began. We delayed the start of scanning till this bright spot faded which required losing almost 25% of the 39 seconds of totality. On the scan to the north of the sun the sky increased in brightness and was brighter than the corona at 3 R_o. On reversal of the scan the sky signals on both recorders, which differed by a factor of 10 in sensitivity, saturated and remained so until after totality. We can only conclude that there were still cumulus fragments moving in the region of the eclipsed sun. On the first half of the first scan coronal brightnesses a factor of two higher than at the 1966 eclipse were recorded. The data from the eclipse provided little new information on dust emission.

The eclipse of March 7, 1970 was observed from Nejapa, Oaxaca, Mexico. Weather on eclipse day was excellent although quite hot. Again a number of difficulties beset us. The worst was the loss of our CO_2 supply which generated only one 4-inch cake of dry ice on eclipse day. Thus the photometer for measurements in the 3 to 5 μ range had to be operated with a hot chopper and with very low sensitivity to obtain on-scale recordings. Only the dual-channel photometer operating with a PIN photodiode and a PbS cell and covering 0.84 to 2.23 μ produced usuable data. Even these were recorded over damped and considerable effort and computer time was required to retrieve the unsmoothed data and then appropriately smooth it.

In addition much effort went into an analysis of the out of focus images of simple lenses since it also appeared that our data were recorded somewhat out of focus. This effort proved unsuccessful and we conclude that the eclipse photometers were in as good focus as simple lenses can provide.

Our experiences with small, low focal ratio, simple lens, photometers at two eclipses lead us to the firm conclusion that such systems are not trustworthy. Thus we, in the future, will use only moderate focal ratio, large-aperture mirror systems in eclipse work. Revision of the light collectors for two dual channel photometers has already begun and will be used at the 1972 eclipse in Canada.

The Mexico eclipse provided sufficient data at 4 R_o to make a first determination of the dust vaporization temperature in that zone. The values obtained from data at 0.84, 1.6, and 2.23 μ yields a temperature 2160±200^{o}K.

The appended paper "A Determination of the Vaporization Temperature of Circumsolar Dust at 4 R_o" was presented at the 135th meeting of the AAS at Amherst, Massachusetts in August 1971 and contains further details of this work.

III. Night Sky and Airglow

The writer has made several attempts to observe the zodiacal light in the near infrared starting with an S-1 cathode photomultiplier tube in 1964. More recently attempts to detect the zodiacal light in the 1.06, 1.6, and 2.2 μ region have been made. Beyond 1 μ the OH airglow becomes very intense and forms a bright background above which the zodiacal light must be detected. So far attempts with wide band filters have been unsuccessful because the airglow is $\sim 10^2$ more intense than the zodiacal light. When a series of measurements were made at 2.2 μ with zero suppression, large irregular patches of OH emission were detected. These patches correspond to cells ~100 km in width. They both vary in brightness and seem to move on the sky. A paper "Airglow Fluctuations at 2.2 μ," co-authored with Lois M. Kieffaber, has recently been accepted for publication in the Journal of Atmospheric and Terrestrial Physics. A copy of the final version is appended. In addition a paper entitled "Twilight and Night Sky Brightness at 2.2 μ" was presented at the 47th AAAS meeting in Tempe, Arizona in April 1971.

Here we showed that infrared twilight ceases at a solar depression angle of about 11° giving hope that infrared measurements of the zodiacal light might extend inward to 15° elongation rather than 20° as in the visible. In addition twilight scans of crepuscular rays (or red twilight rays) were made. These rays are the illumination of the 20 km sulphate aerosol layer by sunlight passing between distant clouds far below the observer's horizon. By timing sunset (i.e., the disappearance) of a ray one can calculate its height. The value obtained for several determinations was 19.5±.5 km which agrees well with other determinations of 20 km.

Satisfying ourselves that wideband photometry with zero suppression, to reveal the small zodiacal light signal, would not work, we have turned to a larger aperture device (a 24-inch searchlight mirror) and to narrow-band cooled, filters ($\Delta\lambda \leq 0.1$ μ) to try and eliminate the OH airglow. This device is just becoming operational and promising test runs have been made. Figure 4 shows two consecutive almucantar scans from Capillo Peak at 1.6 μ and at 2.37 μ. The former contains bright airglow and fluctuations while the latter is presumably almost pure, and steady, thermal emission from the atmsophere. These data show immediately that the OH fluctuations are real and are no doubt due to OH rather than some other airglow mechanism. In addition it seems possible that zero suppression to isolate the small zodiacal light signal riding on a much larger thermal emission signal will now produce data on the zodiacal light.

Future work on the OH airglow fluctuations is also planned as these seem to be due to an entirely different mechanism than

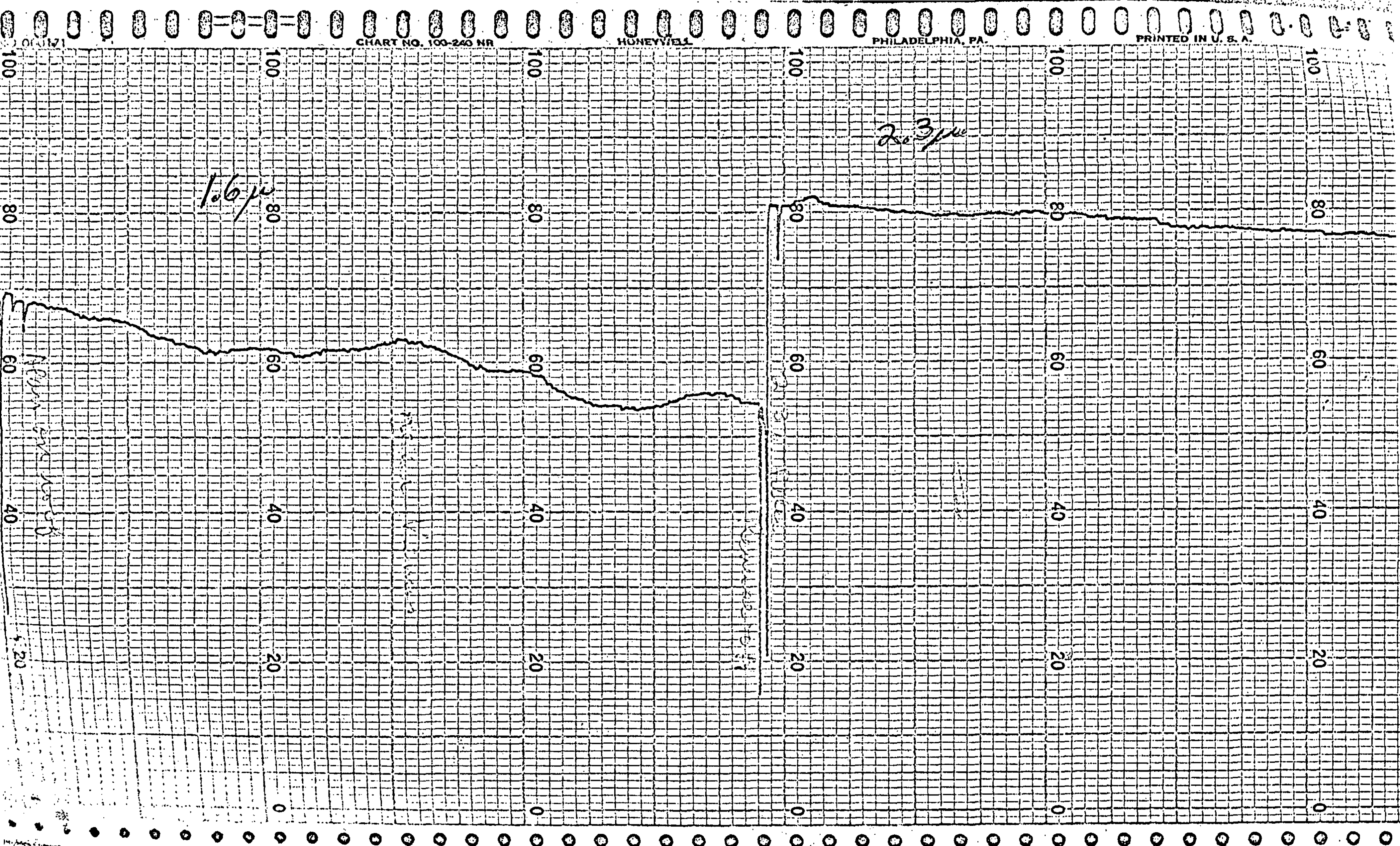

Fig. 4 Consecutive almucantar scans at 6° elevation from Capillo Peak. The first trace is at 1.6 μ and contains OH airglow and large fluctuations; the second trace is at 2.37 μ and contains only steady thermal emission from the atmosphere.

than that which produces the large (~1000 km) patches in the green (O-I) airglow.

IV. Coronal Spectrograph

An experiment to aid in determining the chemical composition of the vaporizing circumsolar dust was conceived and attempted at the 1970 eclipse.

Basically the idea is to look for visual spectral lines due to vapor products from the dust. Sample calculations indicate that the dust vapor will remain near the orbit of the dust particle for a time long compared to the time required for its ionization. This is a period of approximately one day before the vapor is swept out of the corona by the solar wind compared to a period of ~1 hour before electron impacts ionize the atom. Hence an excess of dust vapor ions should be present at the 4 R_o vaporization zone. These are estimated to be nearly as plentiful as inner coronal iron ions, thus they may generate detectable spectral lines.

With these considerations in mind a small fast spectrograph was designed and constructed. It uses a 65 x 76 mm transmission grating and in the first order has a dispersion of 310 Å/mm on a plate photographed by an F = 0.95 Canon camera lens.

Our plates became badly fogged even before the eclipse, presumably due to the intense heat. The plates exposed did show twelve of the known inner coronal lines but the excessive fog prevented detection of any new lines at 4 R_o. This experiment will be repeated at the 1972 eclipse.

The eclipse spectrograph was used to photograph the twilight flash of sodium on several occasions. Since these were the best available plates, to our knowledge, showing this phenomena we wrote up a short article for Sky and Telescope entitled "The Twilight Flash of Sodium," co-authored with Lois M. Kieffaber. A copy of this article is appended.

In addition the spectrograph was modified to work as a slitless instrument in conjunction with our 24-inch F-15 Cassegrain telescope on Capillo Peak. A search of some 30 bright and northerly globular clusters was made in an attempt to find planetary nebulae which might be contained therein. Since only one globular cluster is known which contains a planetary (M15 in Pegasus) it seemed likely that others could be found. So far none has been found. A peculiar star containing Hα emission was detected near a globular. This object does not appear in any list of Hα emitting stars and will be studied further when time permits.

V. Derivative Photometer

A. Dust Emission Zones and the Aureole

A technique common to infrared stellar photometry is the differential, or beam-switching, photometer where the difference in brightness between two areas of the sky produces the output signal rather than having a stationary beam interrupted by a chopper. We have developed a small PbS photometer using this technique in which the beam is switched by one field of view of the detector. The differencing technique should make possible the detection of the 4 R_o thermal emission peak against the day sky background provided the solar aureole is not too bright. Only a few test runs have been made with promising results. It appears that structure in the aureole does exist and that to be successful for daytime dust emission work an observing site such as Haleakala must be used.

B. Intermercurial Objects

A recent revision of the differential photometer permits its use on the 24-inch telescope at Capillo Peak. With this set up we have spent a few hours scanning the region near the sun to search for possible small, hot, intermercurial planets. We estimate that an object 30 km in diameter at 1 A.U. and at 10^{3}°K would be detectable with the differential photometer. Since the field of view of the present instrument is only 6 arc seconds square, this search appears to require a great amount of observing time. On the brighter side we readily detected the planet Mercury only 3 degrees from the sun and with a surprisingly large signal. This work will be persued after the press of the 1972 eclipse lets up.

VI. Personnel

The small size of the program has precluded any full time collaborators.

1. Principal Investigator.

All phases of the program have been under the direct supervision of A. W. Peterson. The majority of the instrumental design, debugging and observing has been performed by him.

2. Others.

E. L. VandeNoord, after receiving his Ph.D. he worked on the project from May 68 to June 69. He collaborated on instrument construction, aircraft observations, 1968 eclipse and data analysis.

Stephanie LaBelle, Data analysis, September 1968 to January 1970.

Lois M. Kieffaber, has cooperated in many phases of the work from January 1970 to the present. She is currently working on the infrared night sky and zodiacal light phase as her Ph.D. research.

David A. Linton, Spring 1970. Mexico eclipse expedition.

Terry Daughtrey, September 1970 to June 1971 - data analysis.

VII. Publications

1. "The Coronal Brightness at 2.23 Microns," Ap. J. 155, 1009, (1969).

2. "Infrared Measurements of the Solar Aureole I. Observations," submitted to J. Atmos. Sci.

3. "Infrared Measurements of the Solar Aureole II. Fraunhofer Diffraction Model," submitted to J. Atmos. Sci. Co-author: E. L. VandeNoord.

4. "The Twilight Flash of Sodium," Sky and Telescope 41, No. 6, (1971). Co-author: Lois M. Kieffaber.

5. "Twilight and Night Sky Brightness at 2.2 Microns," presented at the 47th AAAS Meeting at Tempe, Arizona, April 1971. Co-author: Lois M. Kieffaber.

6. "Airglow Fluctuations at 2.2 Microns," to be published in J. Atmos. Terr. Phys. in 1972. Co-author: Lois M. Kieffaber.

7. "A Determination of the Vaporization Temperature of the Circumsolar Dust at 4 $R_\odot$," presented at 135th Meeting of the AAS, Amherst, Massachusetts, August 1971. (To be submitted to the Ap. J. Letts.)

A Determination of the Vaporization Temperature of Circumsolar Dust at 4 $R_\odot$*

Alan W. Peterson

The University of New Mexico, Albuquerque, New Mexico 87106

At Nejapa, Mexico, an infrared photometry experiment was performed at the total solar eclipse of 7 March 1970 to provide multiwavelength infrared measurements of the circumsolar dust emission predicted by Peterson (1963) and observed independently at 2.2 μ by Peterson (1967) and McQueen (1968) at the 1966 eclipse. The photometers in Fig. 1 made six radial scans out to 10 $R_\odot$, at three position angles. The coronal brightness was recorded at 0.837, 0.96, 1.57, 2.23, 3.53, 3.7, 4.1 and 4.79 μ. Data at the last four wavelengths were unsuitable for analysis because a leak and consequent loss of our high pressure CO_2 supply necessitated operating one dual-channel photometer with a hot, rather than dry-ice cooled, chopper, which greatly compressed the brightness scale of the recordings. In addition, the data at 0.96 μ were of low quality; hence, they too were

*Presented at 135th meeting of the American Astronomical Society, Amherst, Mass., August 24-27, 1971.

rejected. Finally, all data were recorded over-smoothed. Considerable effort has been expended in reprocessing the data to retrieve the unsmoothed data, then resmoothing it at an optimum value of time constant consistent with the field of view and scanning rate.

Our interest lies primarily in the three to five solar radii region where the 1966 observations revealed a strong emission feature at 4 $R_{\odot}$. This feature is interpreted as a region in which circumsolar dust is undergoing rapid vaporization. By fitting two or more brightness measurements at different wavelengths to a Planck curve, the black-body vaporization temperature of the dust can be deduced, and hence a chemical composition for the dust can be inferred.

My calculations of ten years ago reveal the expected behavior of the dust emission when complete vaporization is assumed to occur at a given distance from the sun. Figure 2 shows the predicted brightness as a function of elongation with four sizes of vaporization free zone corresponding to temperature between 900 and 1900°K. When such a curve is added to the coronal brightness, a characteristic peak results, marking the edge of the dust-free zone.

Our eclipse results at three wavelengths and averaged over four radial scans are shown in Fig. 3. Note the emission features at 4 $R_{\odot}$ and that even at 8400 Å significant emission is present. The brightness above the continuum, extrapolated through the bumps, is given in Table I. Notice that maximum emission occurs near 1.57 μ.

Taking the ratio of Planck's formula for two wavelengths and solving for a single temperature, we obtain the values in Table II for each pair of measurements. A value of 2160±200 (rms)$^{\circ}$K results. This is considerably higher than the values near 1000°K suggested for the vaporization of SiO_2 by Over (1958) and Kaiser (1970).

Because the dust composition is unknown, only a dust temperature dependent upon an assumed wavelength-independent albedo can currently be deduced. Table III shows the possible range of temperature for dust at 4 $R_{\odot}$ as a function of albedo. Additional assumptions are that only the sunward side of the non-rotating particle is heated, and that the rotating particle has a uniform surface temperature. The most plausible case would be a particle of small albedo and with uniform surface temperature due to rotation and/or good thermal conductivity. The temperature determined in this experiment is somewhat higher than for a black rotating particle. This may imply a long wavelength infrared emissivity less than unity, possibly due to small particle sizes.

Since the temperature determined is high, we now examine cosmically abundant carbon particles as the possible main elemental constituent of the dust at 4 $R_{\odot}$. Compounds have not been studied yet. Because the early calculations based upon Ingham's model of the zodiacal cloud produced predicted brightnesses a factor of ten higher than observed, it is not inconceivable that fractional vaporization of the dust has occurred farther from the sun (Peterson, 1964). McQueen's balloon observation of emission features at 8.7 and 9.2 $R_{\odot}$ confirm this supposition.

Table IV shows the vapor pressure of graphite for various temperatures, along with the pressure of the ambient coronal gas. It is seen that at a graphite temperature of about 1900°K, the vapor pressure and the ambient pressure of the corona are equal.

However, the relevant question is: What is the vapor pressure of graphite in the presence of the coronal gas at 4 $R_{\odot}$? For it is the vapor pressure which determines the vaporization temperature of a substance in a gaseous environment, and not the temperature which determines the vapor pressure, as Table IV might seem to imply. At 4 $R_{\odot}$, with the usual assumption on dust density ($\sim 5 \times 10^{-21}$ gm/cm^3), the graphite vapor pressure is 10^{-14} atm, which implies a vaporization temperature of about 1650°K. Even graphite would thus vaporize before it could attain a temperature of 2000°K.

This latter inconsistency comes about, we believe, because throughout these calculations, and similar calculations of others, such equations as the "log p" formula relating vapor pressure and temperature make the tacit assumption that the graphite grain and its vapor are in equilibrium. That this is not a valid assumption can be seen from Table V. At 2000°K the vapor leaves the particle with an rms velocity of 2.1 km/sec. Though the coronal electrons have a very high velocity, the collision rate is small, only about 20 per day, so there is no impediment to the immediate escape of the vapor. In addition, those collisions that do occur have the effect of sweeping away the vapor, due to the orbital velocity of the dust particle.

Thus the grain cannot be in equilibrium with its vapor, and any calculations which assume that is is must be suspect. We conclude that because we do not have an equilibrium condition, it is possible for graphite or some other highly refractory material to exist at temperatures of 2000°K at 4 $R_{\odot}$.

Appreciation is expressed to David A. Linton for assistance with the observations, to Terry Daughtrey for assistance with the data reduction, and to Miss Lois M. Kieffaber for her untiring effort during the entire project. This work was supported under the NASA grant NGR 32-004-036 and the NSF grant GA 17291.

References

Kaiser, C. B. 1970, Ap. J., 159, 77.

McQueen, R. M. 1968, Ap. J., 154, 1059.

Over, J. 1958, Proc. Kon. Ned. Akad. Wetenschappen, 51B, 74.

Peterson, A. W. 1963, Ap. J., 138, 1218.

Peterson, A. W. 1964, Ann. N. Y. Acad. Sci., 119, 72.

Peterson, A. W. 1967, Ap. J. (Letters), 148, L37.

Figure 1. Photograph of Eclipse Equipment.
Not Included

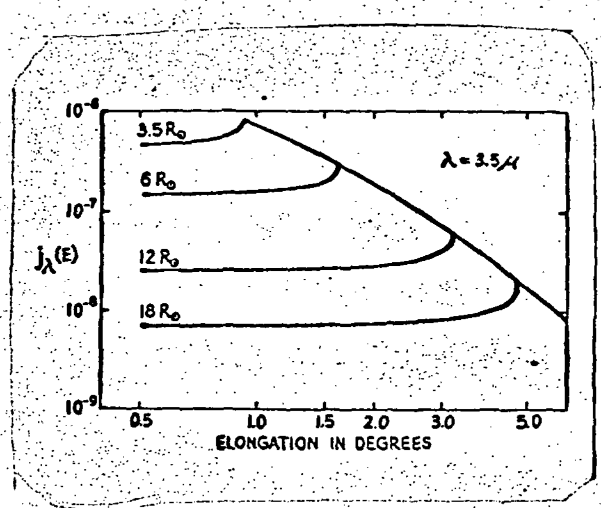

Figure 2

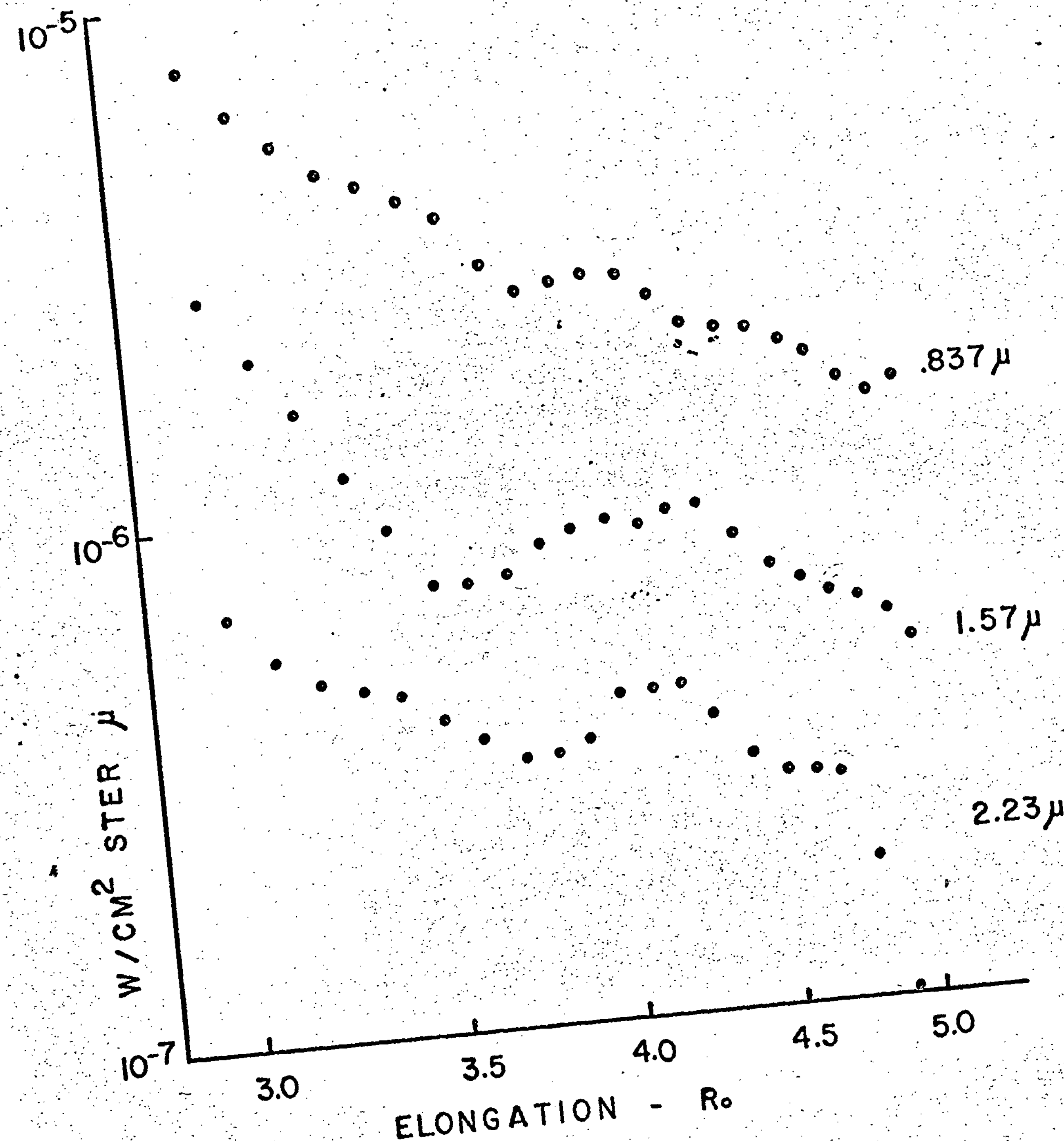

10⁻⁵
10⁻⁶
10⁻⁷
W/CM² STER μ
.837μ
1.57μ
2.23μ
3.0
3.5
4.0
4.5
5.0
ELONGATION - R₀

Figure 3

TABLE I

Observed Emission at Three Wavelengths

Wavelength (μ)	$\Delta B_{\odot}$ (10^{-9})	ΔB (w/cm^2 ster μ)
0.837	.15	2.3×10^{-7}
1.57	1.0	3.1×10^{-7}
2.23	2.0	2.2×10^{-7}

TABLE II

Determination of Vaporization Temperatures

Wavelengths (μ)	Black-body Temperature (^{o}K)
.837 1.57	2330
.837 2.23	2220
1.57 2.23	1940
	Mean 2160 ± 200 (rms) ^{o}K

TABLE III

Dust Temperature as a Function of Albedo at 4 $R_{\odot}$

Albedo	Non-Rotating (°K)	Rotating (°K)
0	2888	2042
.01	2881	2037
.05	2853	2017
.1	2813	1989
.2	2732	1932
.4	2541	1797
.6	2296	1623
.8	1932	1366
.9	1623	1148

TABLE IV

Graphite Vapor Pressure
at Various Temperatures

$\log p = 8.01 - 37100/T$

Temperature (^{o}K)	Vapor Pressure (atm)
2160	6.9×10^{-10}
1960	1.2×10^{-11}
1760	8.7×10^{-12}
1560	1.7×10^{-16}
1460	4.1×10^{-18}

(for solid-vapor equilibrium)

Pressure of the Corona at 4 R_o

$N_e = N_p = 10^5$ cm-3

$p = 2N_ekT = 2.7 \times 10^{-11}$ atm

TABLE V

Orbital Velocity of Particle	$v_{orb} = 4.4 \times 10^7$ cm/sec
Velocity of Escaping Molecules	$v_{vapor} = 2.1 \times 10^5$ cm/sec
Rms Velocity of Coronal Electrons	$v_{elec} = 6.7 \times 10^8$ cm/sec

AIRGLOW FLUCTUATIONS AT 2.2 μ

A. W. PETERSON and L. M. KIEFFABER

Department of Physics and Astronomy, The University of New Mexico

Albuquerque, New Mexico 87106 U.S.A.

(Received ___________)

ABSTRACT

The OH airglow has been observed in the infrared, from high altitude sites, with a bandpass filter from 2.0 to 2.5 μ. An average spatial fluctuation of ±4% and an average time fluctuation of ±3% is found about the mean nightly level. The evening fluctuations are more pronounced than the morning ones. The brightness and fluctuations are such as to preclude ground-based observation of the zodiacal light with wide-band photometry at this wavelength.

1. INTRODUCTION

This study arose as a result of an attempt to observe the zodiacal light in the infrared, as yet unobserved from the ground beyond 1 μ. A comparison of the infrared night sky spectrum and approximate atmospheric transmission, shown in Fig. 1, suggests that in both the 1.6 μ window and the 2.2 μ window a large contribution from airglow can be expected. Airglow measurements have been made at 1.6 μ by HARRISON and VALLANCE JONES (1957), NOXON, HARRISON and VALLANCE JONES (1959), MOROZ (1960), and HUPPI and STAIR (1969). There is fair agreement on the absolute brightness of the airglow at this wavelength. However, data at 2.2 μ are scarce (NOXON et al., 1959; MOROZ, 1960) and show considerable scatter.

We chose the 2.0 to 2.5 μ window as the range promising the least airglow contribution. Beyond 3 μ NOXON et al., found that the thermal emission of the atmosphere is overwhelmingly bright. Since the estimated zodiacal light brightness at 2.2 μ is low (~10^{-10} watt/cm^2 ster μ), a filter with bandpass 0.54 μ covering the entire atmospheric window was used.

Our preliminary measurements showed that airglow brightness at this wavelength much exceeds the expected zodiacal light brightness and in addition contains large fluctuations. Fluctuations were first mentioned by HARRISON and VALLANCE JONES (1957), who reported that OH emission at 1.68 μ is subject to fluctuations during the course of the night and from night to night. We present measurements of the brightness and structure of the night sky at 2.2 μ. Spectra from 1.2 to 2.5 μ obtained by GUSH and BUIJS (1964) with a balloon borne interferometer show that in this region the only significant radiation is due to the 9-7 band of OH.

2. INSTRUMENTATION

A diagram of the instrumentation is shown in Fig. 2. The detector is a Santa Barbara Research Center photoconductive lead sulfide cell, cooled by dry ice. It is located at the focus of a 12-inch f/0.48 reflector. The geometric field of view of the photometer is 1.4 square degrees. An interference filter centered on 2.23 μ limits the bandpass to 0.54 μ. The incoming light is modulated by a 50 Hz tuning-fork chopper. The chopper provides the reference signal for a phase sensitive amplifier permitting detection of a small in-phase signal in the presence of large noise background. The amplified signal is then displayed on a strip chart recorder. Calibration of the photometer is by means of a full-aperture collimator and blackbody with variable temperature controlled to one degree Kelvin.

3. OBSERVATIONS AND ANALYSIS

The data were obtained during an eight month period at Capillo Peak Observatory (altitude 9370 ft) in New Mexico and Haleakala Observatory (altitude 10,200 ft) on Maui, Hawaii. The photometer scanned back and forth over a range of 70° in azimuth at a constant elevation of 6°. The data in Figs. 3 to 5 show typical airglow brightnesses and fluctuations obtained in this study. The arrows indicate the progression of time; the scanning rate was 12° per minute. Figure 3 is representative of an "active" night when pronounced short period fluctuations were observed. The root mean square deviation from the average nighttime brightness is used as a quantitative measure of the magnitude of fluctuations. σ_s will represent the rms <u>spatial</u> fluctuations, that is, fluctuations about the average level over each azimuth scan, shown in Figs. 3 to 5. σ_t will represent the rms fluctuations in time for any one point. These fluctuations can be seen by comparing values along a line of constant azimuth in Figs. 3 to 5. σ will be reserved for the night-to-night fluctuations in the zero-corrected average level. For the evening of 24 January 1971, σ_s = 7.0% and σ_t = 5.0%; for the evening of 2 January 1971, σ_s = 3.7% and σ_t = 2.6%; and for the morning of 3 January 1971, σ_s = 1.2 % and σ_t = 0.9%. The latter was the "quietest" observation period during the study.

The patchiness of the night sky in the infrared is apparent. Certain bright spots (e.g., azimuth 280°, Fig. 3) maintained their identity over times as long as an hour, although the average lifetime is about half an hour (azimuth 245°, Fig. 4). At azimuth 255° in Fig. 3 is a bright patch which faded away, or moved out of the field of view of the photometer, in about 15 minutes. The maximum at azimuth 285° in Fig. 4 is moving south in the sky. The longest-lived feature observed during this study was the small maximum at azimuth 145° in Fig. 5. It remained recognizable for an hour and a half.

The angular length of a "bright cell" is about 10°. If the airglow layer is at 80 km., and we observe at 6° elevation, then the horizontal dimension of such a cell is about 100 km.

We find that the magnitude of the fluctuations is in general higher in the evenings than in the mornings, the average value of σ_s and σ_t being 2.6% and 2.4%, respectively, for mornings and 4.4% and 3.1%, respectively, for evenings. Figures 3 and 4 are evening and morning periods from the same night, and they illustrate this behavior.

We believe that the observed fluctuations cannot be attributed to variations in atmospheric transparency. The data were recorded during very clear nights with no detectable clouds. Furthermore, changing transparency would cause variations in any light traversing the lower atmosphere. Observations of late twilight, which originates in the upper atmosphere, during the same evenings as airglow fluctuations were observed, show no such fluctuations. In addition, atmospheric conditions at the two sites are quite different. Haleakala is several thousand feet above the trade wind inversion layer and atmospheric conditions are thus quite stable. Since comparable fluctuations were observed at both sites, and they were not observed in late twilight, we conclude that they are not due to variations in atmospheric transparency.

HUPPI and STAIR (1969), observing zenith airglow at 37,000 ft with a bandpass filter of 1.4 to 2.0 μ, report a 50% increase in brightness after the minimum following infrared twilight. This maximum occurred at solar depression angle 13°. They also found a predawn minimum at solar depression angles of 10 to 11°. Neither of these phenomena seen at the zenith were observed in our 2.2 μ data taken at 6° elevation.

The problem of determing the background correction for night sky measurements of extended sources still plagues all observers, since a standard method of reduction has not yet been established. At this wavelength the night sky background, i.e., integrated starlight and scattered light from all sources, with the possible exception of zodiacal light, is negligible. In addition, however, we had to contend with a large in-phase signal, presumably due to cross-talk between the reference and the signal channels. Fortunately, airglow increases with decreasing elevation angle, thus providing a means of separating and subtracting the other contributions to the signal. Recent rocket measurements of the OH intensity in the nightglow (PACKER, 1961; BAKER and WADDOUPS, 1961; STAIR and GAUVIN, 1967) have placed the maximum in the 80 to 100 km region. To determine the magnitude of an appropriate zero correction, we performed many scans in elevation. We then compared the average of these scans with a Van Rhijn curve for an 80 km emitting layer. The zero correction was taken as that value which brought the observed ratios of brightness at various elevation angles into agreement with the Van Rhijn curve. This seemed an appropriate technique because (1) the zero correction was found to be constant for a given night, (2) there was a linear relationship between the zero correction and the average level of the total signal, and (3) the total signal strength varied widely from night to night (rms deviation 89%), while after subtracting the zero correction determined by fitting to a Van Rhijn distribution, the rms deviation dropped to $\sigma = 15\%$. All data presented have had such a zero correction.

Figure 6 shows a typical scan in elevation. A Van Rhijn curve for a uniform emitting layer at 80 km is shown for comparison. The extinction coefficient of 0.05 at 2.2 μ was determined by measuring the brightness as a function of altitude for stars with large negative K-magnitudes. The airglow "layers" seen here are typical of the structure observed in altitude scans on active nights. On this particular evening the enhancement between 30° and 55° elevation angle remained for more than 45 minutes.

The average of the airglow brightness during an entire night varied from night to night. The average of the nightly values during the period of this study was $(13 \pm 2) \times 10^{-9}$ w/cm^2 ster μ at elevation angle 6° and filter bandpass of 0.54 μ.

A comparison with values of other observers would be of interest; each observer, however, works at a particular zenith angle and a particular instrumental bandpass, so direct comparison of their numbers is not meaningful. In Table I appears our attempt at a meaningful comparison. First, the observations of NOXON et al., and the present study are corrected to the zenith. For the former, a Van Rhijn ratio for a uniform layer at 80 km, uncorrected for extinction, was used. For the latter we used our own zenith measurements.

Secondly, we have the problem of differing instrumental bandpasses. To normalize all the observations for purposes of comparison, the following technique was used:

$$\text{Normalized brightness of entire band} = \text{Observed brightness corrected to zenith} \cdot \left[\frac{\text{Instrumental bandpass}}{\text{Normalizing bandwidth}}\right]$$

or

$$B_n = B_o \frac{\Delta\lambda_i}{\Delta\lambda_n}$$

This is a straightforward normalization for the wide-band instruments. For the spectral measurements of HARRISON and VALLANCE JONES, NOXON et al., and MOROZ, the quantity of $B_o \Delta\lambda_i$ is the integrated brightness over the emission band. For a normalizing bandwidth $\Delta\lambda_n$, we chose to use widths derived from rectangular approximations of the emission bands with an average brightness equal to that seen by NOXON et al. They are $\Delta\lambda_n = 0.3\ \mu$ for the 1.6 μ band and $\Delta\lambda_n = 0.15$ for the 2.2 μ band.

It is seen from the results of this comparison that there is fair agreement on the brightness of the 1.6 μ band. At 2.2 μ the present measurement is in better agreement with the value reported by NOXON et al., than that of MOROZ.

4. CONCLUSIONS

After zero correction, the OH airglow at 2.2 μ is found to vary in average level from night to night with $\sigma = 15\%$. During any given night space fluctuations are present, having $\sigma_s = 6$ to 7% on active nights and 1 to 2% on quiet nights, and time fluctuations with $\sigma_t = 4$ to 5% on active nights and 0 to 1% on quiet nights. The overall averages are $\sigma_s = \pm 4\%$ and $\sigma_t = \pm 3\%$. We conclude that the fluctuations are intrinsic to the airglow and are not due to variations in atmospheric transparency. On active nights the peak-to-peak spatial fluctuations are larger by at least a factor of ten than the expected zodiacal light brightness. Thus the OH airglow precludes the possibility of observing the zodiacal light at this wavelength with ground-based wide-band photometry. On a given night the evening fluctuations are larger than those observed in the morning. It would be of considerable interest to study an extended series of OH fluctuation measurements for possible correlation with geomagnetic or solar activity.

ACKNOWLEDGEMENTS

The research reported here was made possible by NASA Grant NGR-32-004-036. Special thanks are due to Professor J. B. Zirker of the University of Hawaii for use of facilities at Haleakala Observatory and to Terry Daughtrey for help in data reduction.

REFERENCES

BAKER, D. J. and WADDOUPS, R. O. 1961 Quarterly Status Report No. 3 Contract No. AF19 (628)-5916 Utah State University

GUSH, H. P. and BUIJS, H. L. 1964 Can. J. Phys. 42, 1037

HARRISON, A. W. and VALLANCE JONES, A. 1957 J. Atmosph. Terr. Phys. 11, 192

HUPPI, E. R. and STAIR, A. T., Jr. 1969 Atmospheric Emissions (Edited by B. M. McCormac and A. Omholt) pp. 471-5. Reinhold, New York

MOROZ, V. I. 1960 Astron. Zh. 37, 123

NOXON, J. F., HARRISON, A. W. and VALLANCE JONES, A. 1959 J. Atmosph. Terr. Phys. 16, 246

PACKER, D. M. 1961 Ann. Geophys. 17, 67

PLASS, G. N. and YATES, H. W. 1965 Handbook of Military Infrared Technology (Edited by W. L. Wolfe) p. 252. Office of Naval Research, Washington, D. C.

STAIR, A. T., Jr. and GAUVIN, H. P. 1967 Aurora and Airglow (Edited by B. M. McCormac) p. 383. Reinhold, New York

FIGURE CAPTIONS

Figure 1. Spectrum of the night sky from 1.5 to 3.0 μ at zenith angle 80^{o} according to NOXON *et al.*, (1959). They attribute the peaks at 1.6 and 2.2 μ to OH bands, and the increase beyond 2.5 μ to thermal emission of the atmosphere. Relative atmospheric transmission for a 0.3 km sea level path with 5.7 mm precipitable water (PLASS and YATES, 1965) is also shown, as it is a fair approximation of our clear-sky zenith conditions where the amount of precipitable water is typically 1 to 3 mm.

Figure 2. Optical system and electronics of photometer.

Figure 3. Airglow surface brightness as a function of azimuth and time on 24 January 1971 at Capillo Peak Observatory. Rms variations in space and time are $\sigma_s = 7.0\%$ and $\sigma_t = 5.0\%$.

Figure 4. Airglow surface brightness as a function of azimuth and time on 3 January 1971 at Haleakala Observatory. Rms variations in space and time are $\sigma_s = 3.7\%$ and $\sigma_t = 2.6\%$.

Figure 5. Airglow surface brightness as a function of azimuth and time on 3 January 1971 at Haleakala Observatory. Rms variations in space and time are $\sigma_s = 1.2\%$ and $\sigma_t = 0.9\%$.

Figure 6. Typical scan in altitude, recorded 24 January 1971, showing airglow surface brightness as a function of elevation angle. Also shown is a Van Rhijn curve for a uniform emitting layer at 80 km, multiplied by an extinction factor with a measured extinction coefficient of 0.05.

Table I. Measurements of airglow surface brightness

($\times 10^{-9}$ w/cm^2 ster μ)

At 1.6 μ

Observer	Zenith Angle	Instrumental Bandpass $\Delta\lambda_i$	Observed Brightness	Brightness Corrected to Zenith	Normalized Brightness
HARRISON and VALLANCE JONES (1957)	80°	0.02 μ	-	15	12
NOXON, HARRISON and VALLANCE JONES (1959)	80°	0.03 μ	73	17	16
MOROZ (1960)	72°	0.04 μ	-	3.3	3.0
HUPPI and STAIR (1969)	0°	0.6 μ	5	5	10

At 2.2 μ

Observer	Zenith Angle	Instrumental Bandpass $\Delta\lambda_i$	Observed Brightness	Brightness Corrected to Zenith	Normalized Brightness
NOXON, HARRISON and VALLANCE JONES (1959)	80°	0.03 μ	35	8.1	9.3
MOROZ (1960)	72°	0.04 μ	-	0.24	0.20
PRESENT WORK (1971)	84°	0.54 μ	13±2	3.2	12±2

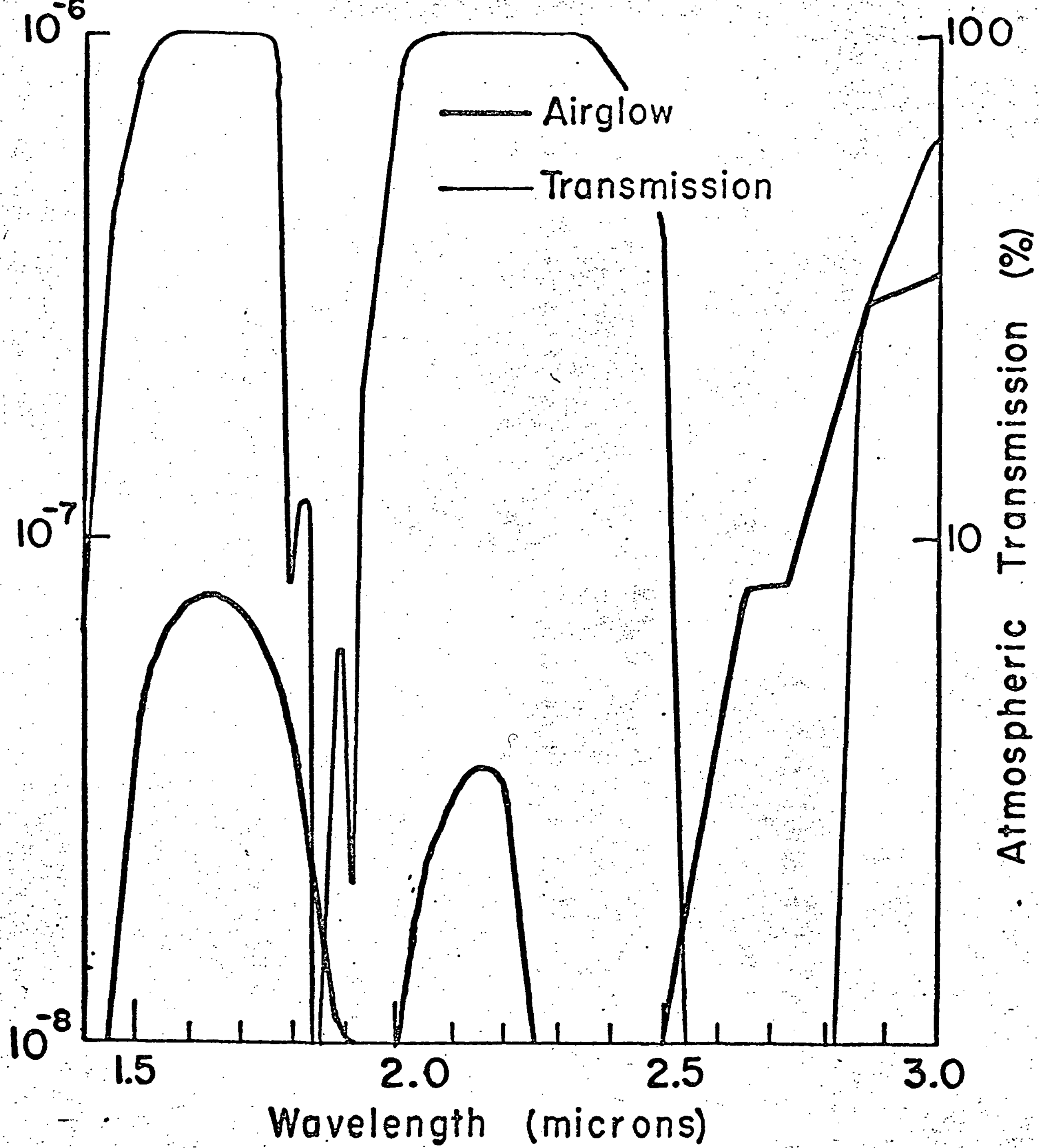

10^-6
10^-7
10^-8
100
10
Airglow
Transmission
Watt/cm² ster μ
Atmospheric Transmission (%)
1.5
2.0
2.5
3.0
Wavelength (microns)

Figure 1

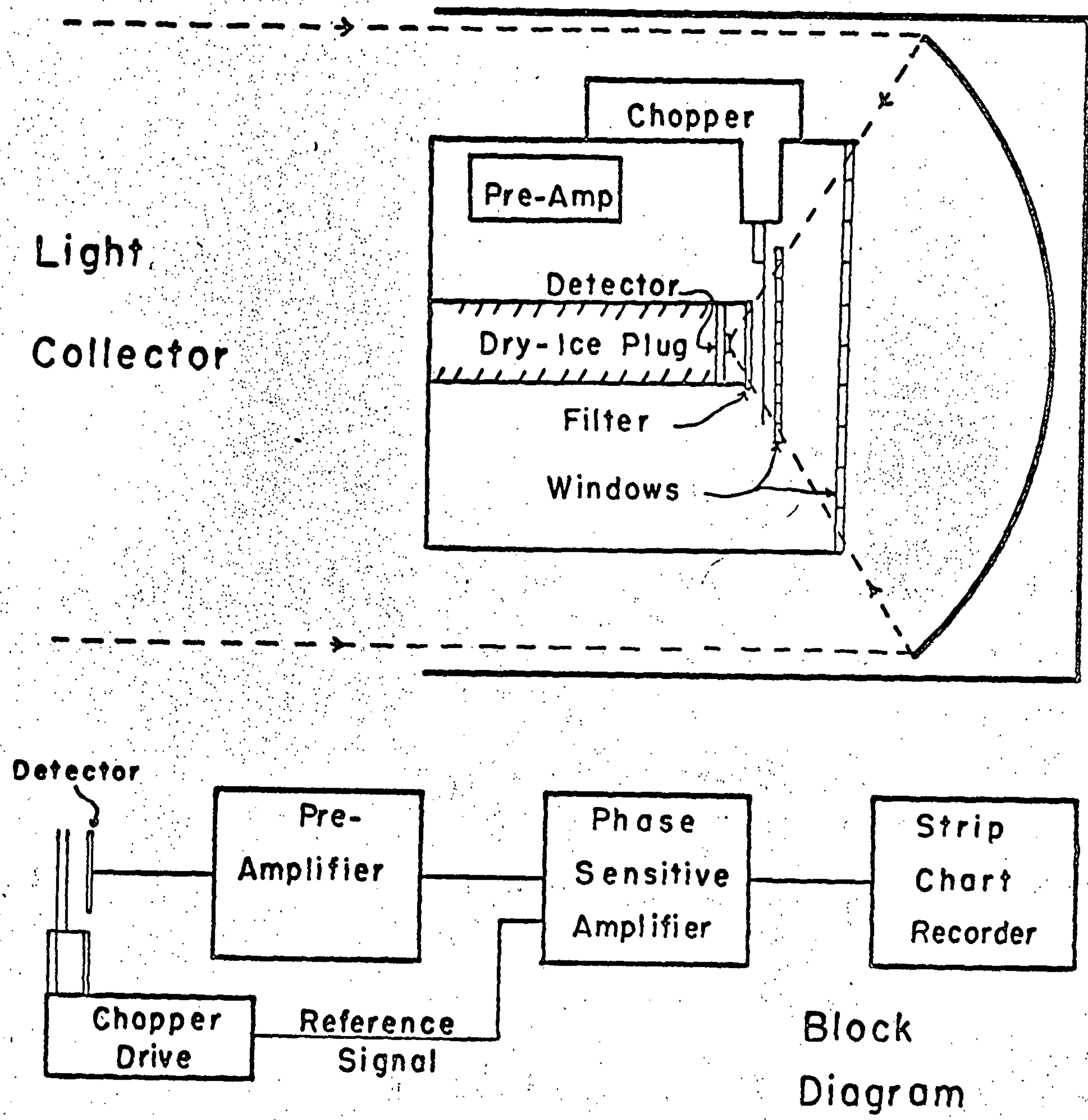

Light Collector
Chopper
Pre-Amp
Detector
Dry-Ice Plug
Filter
Windows
Detector
Pre-Amplifier
Phase Sensitive Amplifier
Strip Chart Recorder
Chopper Drive
Reference Signal
Block Diagram

Figure 2

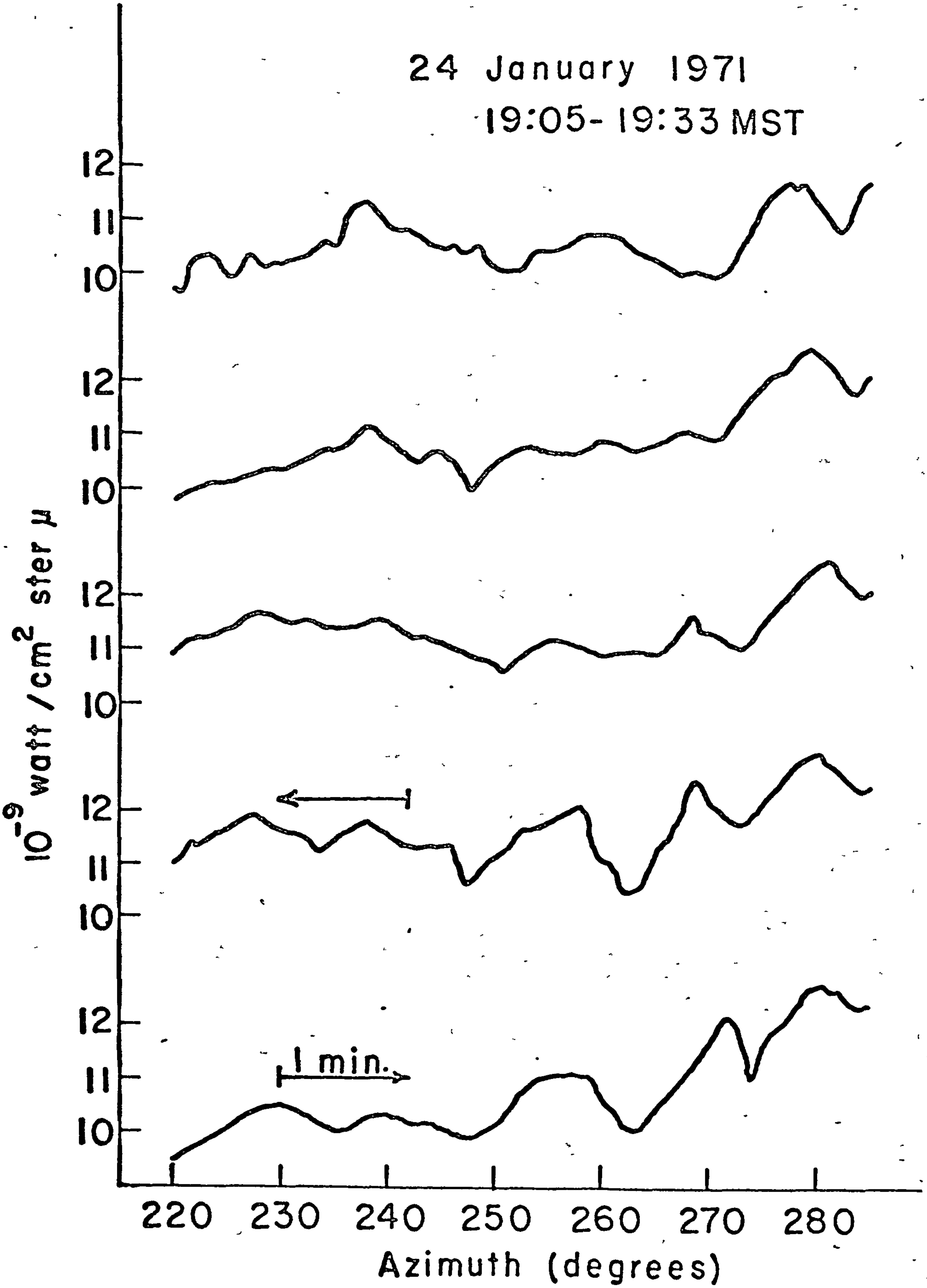
24 January 1971
19:05- 19:33 MST
12
11
10
12
11
10
12
11
10
12
11
10
12
11
10
1 min.
10^{-9} watt /cm^2 ster μ
220
230
240
250
260
270
280
Azimuth (degrees)

Figure 3

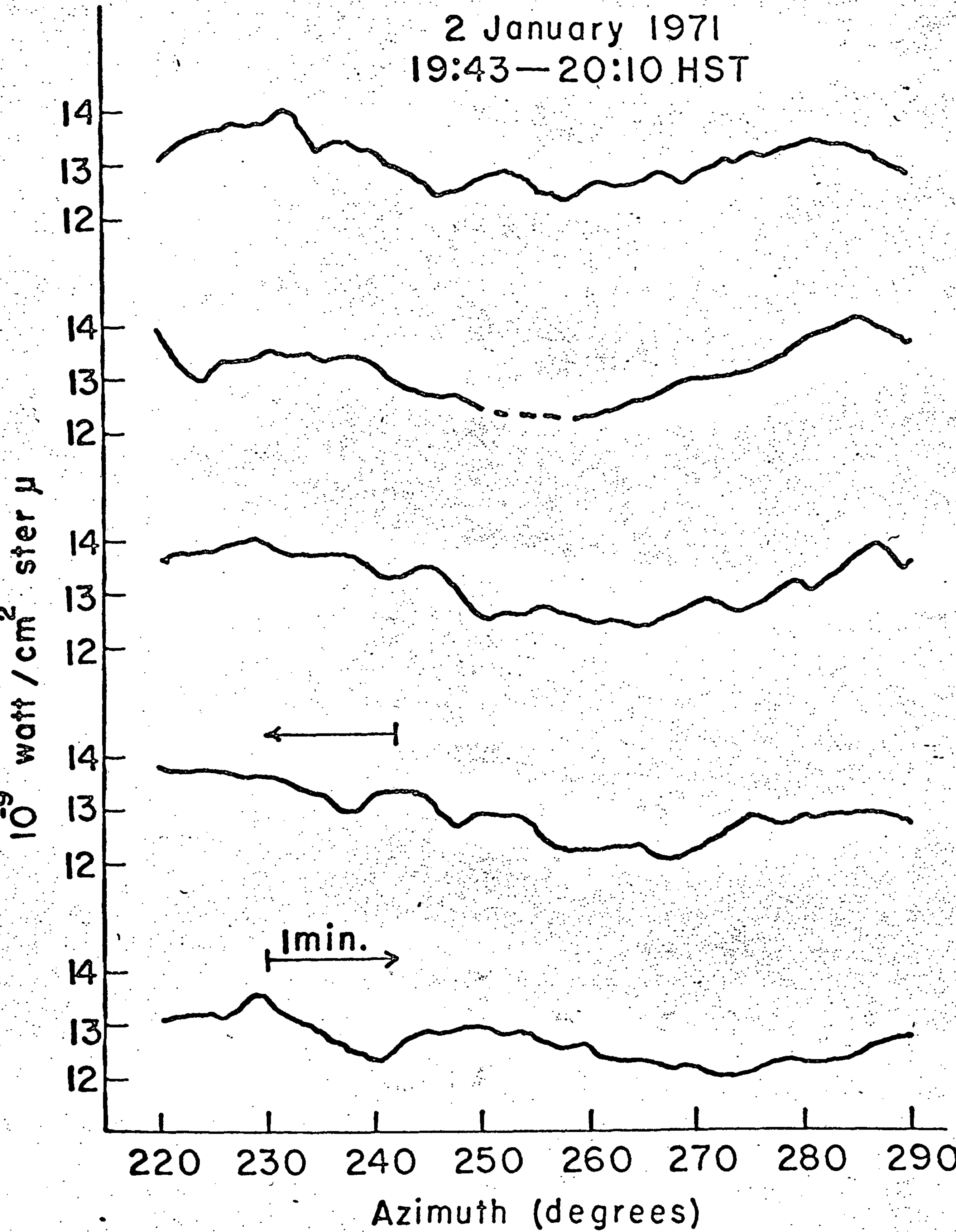
2 January 1971
19:43—20:10 HST
14
13
12
1min.
10^{-9} watt / cm^2 ster μ
220
230
240
250
260
270
280
290
Azimuth (degrees)

Figure 4

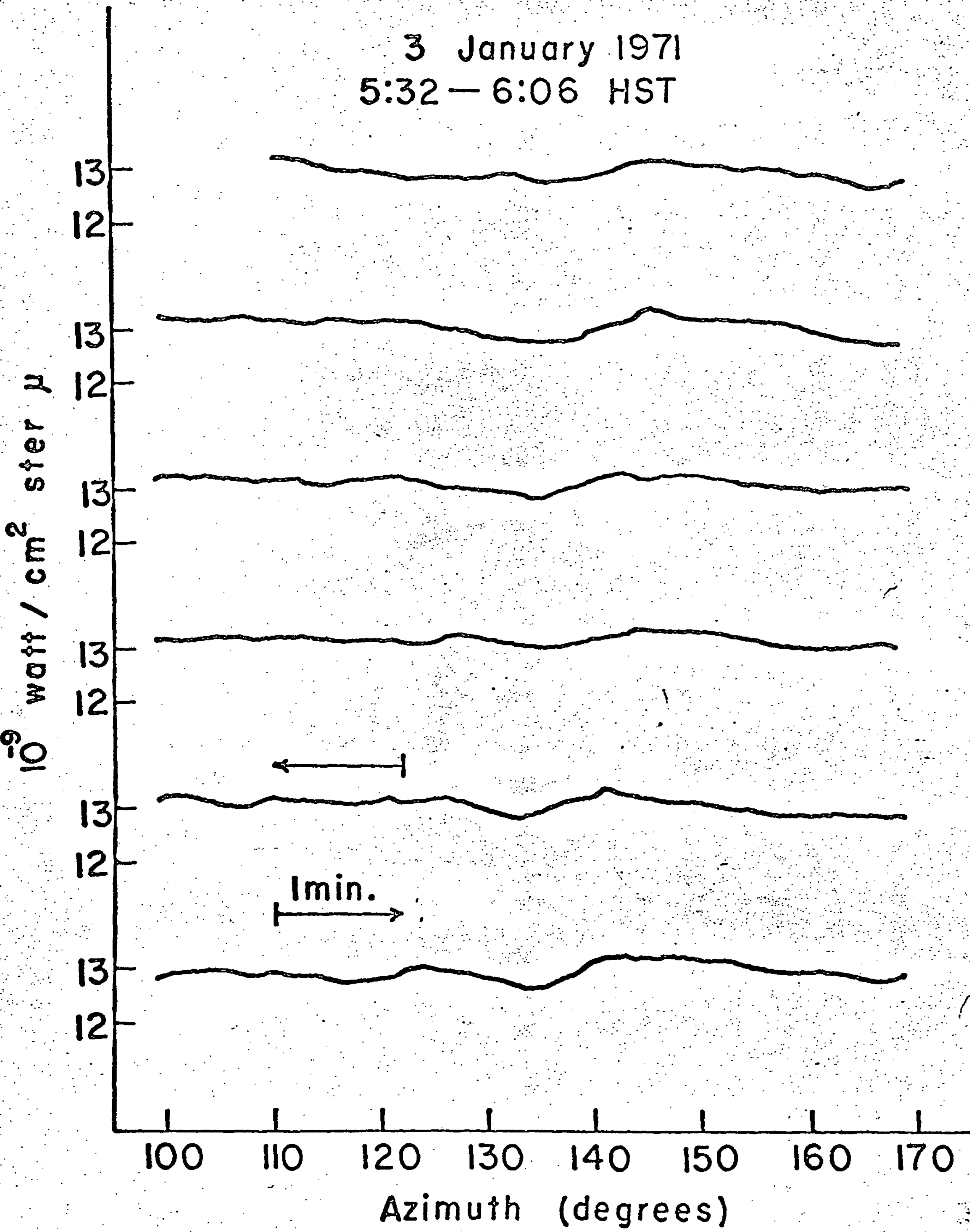
3 January 1971
5:32 — 6:06 HST
10^{-9} watt / cm^2 ster μ
13
12
1min.
100
110
120
130
140
150
160
170
Azimuth (degrees)

Figure 5

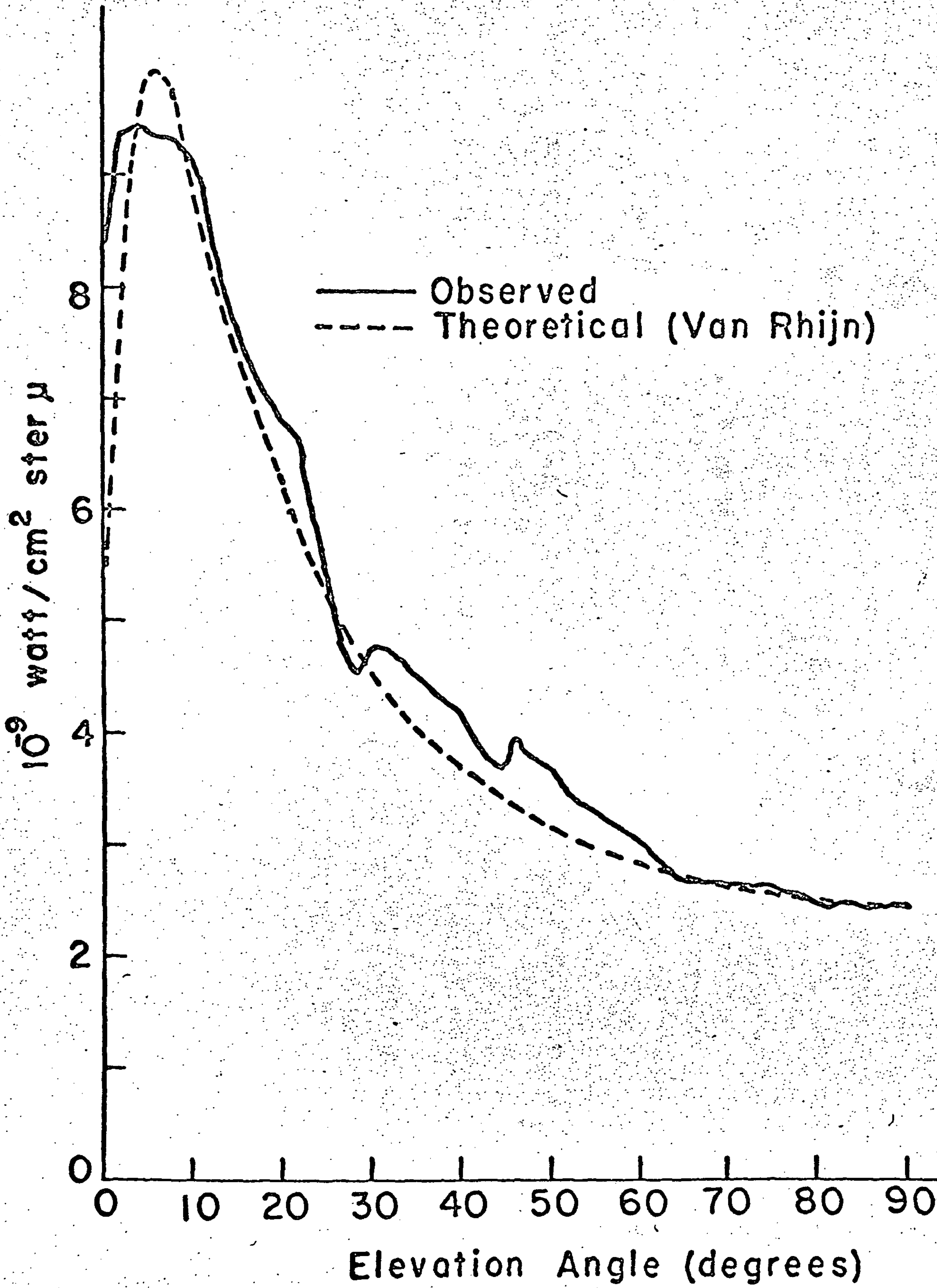

Observed
Theoretical (Van Rhijn)
10^{-9} watt/cm^2 ster μ
0
2
4
6
8
0
10
20
30
40
50
60
70
80
90
Elevation Angle (degrees)

Figure 6

The Twilight Flash of Sodium

ALAN W. PETERSON and LOIS M. KIEFFABER

University of New Mexico

Reprinted from SKY AND TELESCOPE, Vol. 41, No. 6, *June, 1971.*

The Twilight Flash of Sodium

ALAN W. PETERSON and LOIS M. KIEFFABER
University of New Mexico

THE EXISTENCE of atomic emission lines originating in the earth's ionosphere has been known for many years. The familiar green line at a wavelength of 5577 angstroms, arising from atomic oxygen, was first detected visually in 1895, with a spectroscope by W. W. Campbell at Lick Observatory. In 1919 this line was rediscovered photographically by V. M. Slipher at Lowell Observatory. (Molecules as well as atoms are now known to contribute to this continual emission of the clear night sky, the *airglow.)*

In 1928 Slipher detected the red oxygen lines near 6300 angstroms, as well as the yellow sodium doublet at 5893. The latter was not conclusively identified as being due to sodium until 1938, when R. Bernard observed it in the twilight sky. Similar studies were performed by J. Cabannes, J. Dufay, and J. Gauzit.

In spite of Slipher's comment that the yellow airglow line had a wavelength close to that of the sodium D doublet, the idea of free metal atoms in the atmosphere did not seem too plausible. However, interferometer measurements of the exact wavelength established the identity of the emitting atoms. The source of these sodium atoms, whether terrestrial from sea water or vulcanism, or celestial from meteoric debris, remains unclear.

Spectral lines of calcium and potassium (an alkali element, like sodium) have also been found in the twilight glow. More recently, lithium emission resulting from thermonuclear weapons testing has made its appearance. Gas of any alkali metal is a very effective scatterer of radiation that has the same frequency as the natural or resonant frequency of the single valence electron.

As the diagram for sodium shows, this valence electron exists outside the other completely filled shells of electrons. Because of the electron property known as spin, the excited level is double, and the resonance emission spectra of the alkali metals consist of pairs of lines with slightly different wavelengths. And since the electron is loosely bound to the atom, the resonance frequency is in the visible region of the spectrum, making possible a very interesting effect — the twilight flash of the yellow sodium lines.

For just a few minutes, the sodium lines are very much brighter than the nearby continuous spectrum that results from direct sunlight being scattered by the atmosphere. At that time, the lines are also greatly enhanced over their nighttime airglow brightness.

To appreciate how the twilight flash occurs, we note first that the sodium atoms are confined to a relatively narrow layer high in the atmosphere. The peak concentration occurs at 90 kilometers and the layer is some 20 kilometers thick.

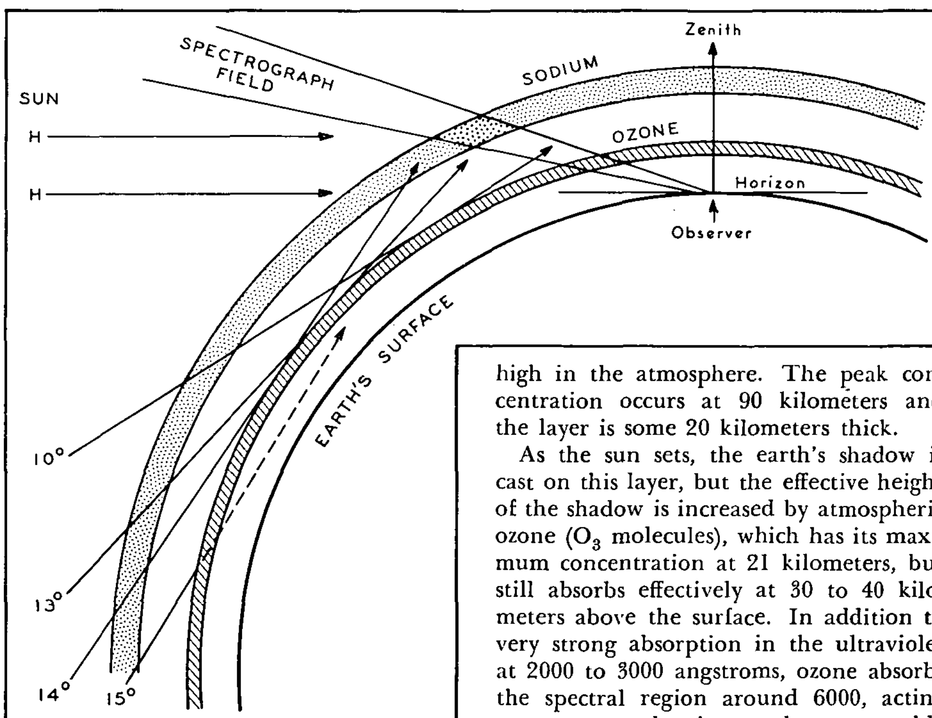

A schematic representation of the geometry of sunset. Direct illumination of the sodium layer occurs until the sun is 13° below the horizon, when screening by the ozone layer begins.

As the sun sets, the earth's shadow is cast on this layer, but the effective height of the shadow is increased by atmospheric ozone (O_3 molecules), which has its maximum concentration at 21 kilometers, but still absorbs effectively at 30 to 40 kilometers above the surface. In addition to very strong absorption in the ultraviolet at 2000 to 3000 angstroms, ozone absorbs the spectral region around 6000, acting as an opaque barrier to photons capable of exciting the sodium doublet.

In the diagram showing the geometry of post-sunset events in the sodium layer, the heavy stippling represents the region viewed by a spectrograph pointed to the western sky at a zenith angle of about 75 degrees. Arrows H indicate sunset rays, which strongly illuminate the lower atmosphere through which the spectrograph is directed. Until the sun is at least 8° below the horizon, all emissions by the atmosphere are overwhelmed by the bright scattered sunlight; hence only absorption lines originating in the sun are visible.

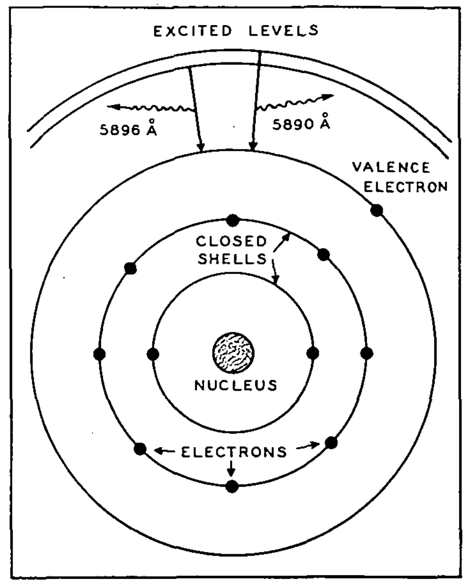

In the sodium atom, the valence electron can make two transitions that give rise to a closely spaced pair of emission lines. In absorption, the valence electron jumps up to the excited levels.

As twilight deepens, only higher and higher levels of the atmosphere are illuminated from below. When the sun's depression is about 10°, the sodium absorption line suddenly disappears! The doublet at 5893 angstroms becomes completely filled in by photons of the same wavelength scattered by atoms of atmospheric sodium.

Scattering by the sodium layer remains constant while the total atmospheric scattering diminishes. Hence the sodium emission increases rapidly in intensity relative to the adjoining continuum and the sodium flash ensues (11° and 12°). When direct sunlight is cut off at all levels below the sodium layer (13°), the emission lines attain their maximum brightness, about 10 times that of the continuum.

As the sun descends further, the sodium emission itself weakens (14°). Finally, it disappears when the sun is about 15° below the observer's horizon, due to complete cutoff by the ozone layer. A very weak sodium line is seen in the spectrum of the night airglow, but this arises from a different mechanism than resonance scattering, and it is present all night. At morning twilight the sodium flash occurs again, but with events in reverse order as the sun illuminates lower and lower layers of the atmosphere.

Observations of the flash have been conducted with some success here at the University of New Mexico as an undergraduate astronomy laboratory experiment. Although built for another purpose, a grating spectrograph has performed well. It has a fast camera lens (f/0.95) and a linear dispersion of 310 angstroms per millimeter.

The typical twilight-flash spectral sequence reproduced here was taken April 27, 1970, on open ground several miles west of Albuquerque at about 6,000 feet above sea level. Although the city was below our horizon, its mercury-vapor streetlights still produced strong contamination, including the bright line at 4358 angstroms. Local sunset was at 19:36 Mountain daylight time, when the sun's hour angle was 99°.4. For each frame the table gives the solar depression, hour angle, time, minutes after sunset, and the length of exposure in seconds.

KEY TO PHOTOGRAPHS

Sun's Dep.	*H.A. (°)*	*Time (MDT)*	*Sunset (min.)*	*Exp. (sec.)*
8°	109.8	20:18	+42	8
10°	112.5	20:27	+51	15
11°	113.9	20:33	+57	50
12°	115.2	20:38	+62	75
13°	116.6	20:42	+66	180
14°	118.0	20:46	+70	300
15°	119.3	20:53	+77	900

In the first exposure the typical solar spectrum is evident, but much overexposed except from about 5300 to 6300 angstroms, where ozone absorption already present reduces its intensity. The sodium doublet appears as an absorption line, but it has disappeared in the picture for 10°, for the reason explained above.

Only six minutes later the sodium line appears prominently in emission (11°), and at 12° and 13° it is the brightest line in the twilight spectrum. On our negatives, the red oxygen line at 6300 angstroms appears at 11°, the green oxygen line (5577) at 12°. And even with the twilight sky still rather bright, mercury contamination has set in.

By the sixth frame, with the sun 14° below the observer's horizon, the sodium flash has subsided, indicating that the ozone layer is screening sunlight from that portion of the sodium layer at which the spectrograph is directed. The oxygen lines are strong and mercury contamination is seen, appearing bright even in the blue end of the spectrum where the ozone absorption is too weak to suppress the scattered solar spectrum entirely. The Fraunhofer G blend at 4307 angstroms appears here in absorption, with the bright mercury feature alongside it.

This shows strongly in the last frame, as do other mercury lines and the oxygen emission. The red line will slowly decrease in brightness to a minimum near local midnight. In general the green oxygen line shows little twilight enhancement. Instead it varies during the night, with no set pattern.

For our undergraduate laboratory experiment, we normally do not inquire further into the details of what may be learned from twilight-flash observations. However, three important results can be obtained: the height of the emitting layer, its thickness, and the number of sodium atoms contained in a column of unit cross section through the emitting layer. Briefly, one would proceed as follows.

When the twilight flash begins, the solar rays are tangent to the top of the ozone layer and they intersect the lower edge of the sodium layer. At the end of the flash, the solar rays just touch the top of the sodium layer. In each case the height of the ray can be calculated, and the thickness of the sodium layer is the difference of the two heights.

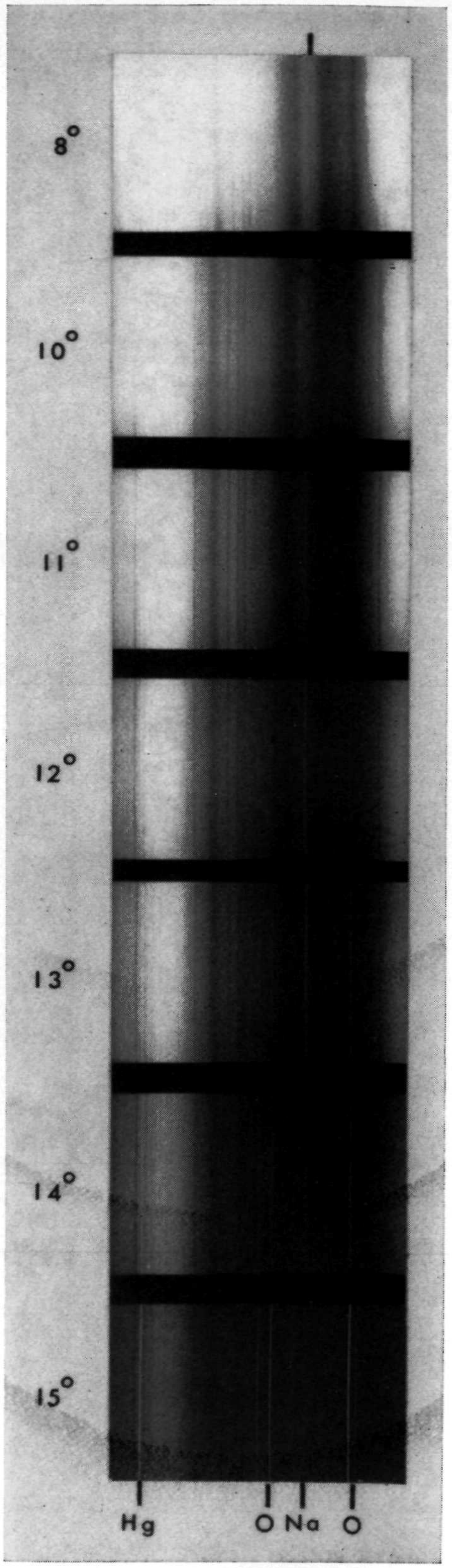

The authors' twilight sequence shows the change of the evening sky from an absorption-line spectrum to one with several conspicuous emission lines.

Deducing the number of sodium atoms in the unit column is more complicated. The photographic plate must be calibrated with a standard lamp of accurately known spectral energy distribution. Then the amount of blackening of the plate by the sodium lines permits an estimation of the number of sodium-line photons emitted by the layer. Comparing this number with the scattering efficiency of sodium atoms and with the amount of solar illumination at the wavelength in question allows us to evaluate the number of sodium atoms present in the column. The result is between 5×10^9 and 10^{10} atoms in a column one square centimeter in cross section.

Amateur spectroscopists who wish to observe this phenomenon will discover that exposure lengths are very important. One must calculate in advance the times when the sun reaches the specified depression angles. This is done by computing, with spherical trigonometry, the hour angle of the sun at sunset and at each depression angle. The difference in hour angle (expressed in time units) is then added to the time of local sunset. Numbers from such computations are given in the key to the photographs.

The exposure times in that key are for Eastman 098-02 red-sensitive emulsion and an f/0.95 camera lens. With Tri-X emulsion the exposures must be quadrupled. If a slower lens is used, the exposure times must be multiplied by the square of the ratio of f numbers; thus, with an f/2 lens the exposures should be increased by a factor of 4.4. Adopting a prism instead of a grating as the dispersing element would increase speed considerably, owing to greater transmission and lower dispersion.

Because the airglow lines are widely spaced in wavelength, a camera lens of rather poor definition can be tolerated. One of the readily available surplus eyepieces with speeds around f/1 could be used. In any event, the prism or grating must be large enough to fill the camera lens aperture completely.